A two-hit epistasis model prevents core genome disharmony in recombining bacteria

Aidan J. Taylor[1]†, Guillaume Méric[2]†‡, Koji Yahara[3], Ben Pascoe[2], Leonardos Mageiros[2], Evangelos Mourkas[2], Jessica K Calland[2], Santeri Puranen[4], Matthew D. Hitchings[5], Keith A. Jolley[6], Carolin M. Kobras[1], Nicola J. Williams[7], Arnoud H. M. van Vliet[8], Julian Parkhill[9], Martin C. J. Maiden[6], Jukka Corander[4,10,11], Laurence D Hurst[2], Daniel Falush[12], Xavier Didelot[13], David J. Kelly[1*], Samuel K. Sheppard[2,6*]

Affiliations

[1]School of Biosciences, University of Sheffield, Sheffield S10 2TN, United Kingdom;

[2]The Milner Centre for Evolution, Department of Biology and Biochemistry, University of Bath, Bath BA2 7AY, UK;

[3]Antimicrobial Resistance Research Centre, National Institute of Infectious Diseases, Tokyo, Japan;

[4]Department of Mathematics and Statistics, Helsinki Institute for Information Technology, University of Helsinki, Helsinki, Finland;

[5]Swansea University Medical School, Institute of Life Science, Swansea SA2 8PP, UK;

[6]Department of Zoology, University of Oxford, 11a Mansfield Road, Oxford OX1 3SZ, UK;

[7]Department of Epidemiology and Population Health, Institute of Infection & Global Health, University of Liverpool, Leahurst Campus, Wirral, UK;

[8]School of Veterinary Medicine, University of Surrey, Guildford GU2 7AL, UK;

[9]Department of Veterinary Medicine, University of Cambridge, Madingley Rd, Cambridge CB3 0ES, UK;

[10]Department of Biostatistics, University of Oslo, Oslo, Norway;

[11]Parasites and Microbes, Wellcome Sanger Institute, Cambridge, UK;

[12]The Centre for Microbes, Development and Health, Institut Pasteur of Shanghai, Shanghai, China;

[13]School of Life Sciences and Department of Statistics, University of Warwick, Coventry CV4 7AL, UK.

*Corresponding author(s): David J. Kelly, d.kelly@sheffield.ac.uk; Samuel K. Sheppard, s.k.sheppard@bath.ac.uk;

‡Present address: Cambridge Baker Systems Genomics Initiative, Baker Heart and Diabetes Institute, 75 Commercial Rd, Melbourne 3004, Victoria, Australia.

† Contributed equally.

Abstract

Recombination of short DNA fragments via horizontal gene transfer (HGT) can both introduce beneficial alleles and create disharmony in coadapted genomes (negative epistasis). Owing to a lack of protracted intragenomic co-evolution, negative epistatic costs of HGT into non-core (accessory) bacterial genomes are likely to be minimal. By contrast, for the core genome, recombination is expected to be rare because disruptive allelic replacement is likely to introduce negative epistasis. Why then is homologous recombination common in the core of bacterial genomes? To understand this enigma, we take advantage of an exceptional model system, the common enteric pathogens *Campylobacter jejuni* and *Campylobacter coli*, that are known for very high magnitude interspecies gene flow in the core genome. As expected, HGT does indeed disrupt co-adapted allele pairings (negative epistasis). However, multiple HGT events enable recovery of the recipient genome's co-adaption between the alleles, even in core metabolism genes (e.g. formate dehydrogenase). These findings demonstrate that, even for complex traits, genetic coalitions can be decoupled, transferred and independently reinstated in a new genetic background. There is a strong resemblance to the two-hit cancer model. Whether it be by multiple mutations or multiple HGT events, immediate harmful effects from an initial event need not preclude adaptive evolution. The fitness peak jumping problem in asexual lineages is thus less of problem than envisaged.

Introduction

Mutation is the engine of genetic novelty, but for most bacteria adaptation also involves the acquisition of DNA from other strains and species through horizontal gene transfer (HGT)[1]. In some well documented cases, a single nucleotide substitution or acquisition of a small number of genes, can prompt new evolutionary trajectories with striking outcomes such as the evolution of virulent or antibiotic resistant strains[2]. With such dynamic genomic architecture, it may be tempting (and possibly useful[3]) to consider genes as independent units that 'plug and play' innovation into recipient genomes. This is clearly an oversimplification. In fact, genomes are highly interactive wherein the effect of one allele depends on another (epistasis). Therefore, it is likely that some horizontally introduced changes will disrupt gene networks and be costly to the original coadapted genetic background, especially for complex phenotypes involving multiple genes.

Understanding how epistasis influences the evolution of phenotype diversity has preoccupied researchers since the origin of population genetics[4-10], with much emphasis placed upon the relative amounts of recombination and epistatic effect sizes[11, 12]. In sexual populations, such as outbreeding metazoans, genetic variation is shuffled at each generation. As a consequence of the trend towards randomization between alleles (linkage equilibrium) it is unlikely that multiple distinct epistatic allele combinations will be maintained in the same population and barriers to gene flow, such as geographic isolation, may be required for marked phenotypic diversification [8]. In bacteria, rapid clonal reproduction allows multiple genomically distant beneficial allele combinations to rise to high frequency in a single population. For example, in common enteric bacteria such as *Escherichia coli*, *Salmonella enterica* and *Campylobacter jejuni* the doubling

time in the wild has been estimated at around 24 hours or less[13, 14]. Therefore, though HGT occurs in these organisms[15], even in highly recombinogenic *C. jejuni*[13, 16], there will likely be many millions of bacterial generations between recombination events at a given locus. This allows mutations that are beneficial only in specific genetic backgrounds to establish in a single population and linkage disequilibrium to form between different epistatic pairs[17].

In a coadapted genomic landscape, recombination is expected to have two antagonistic effects. On the one hand, it could promote adaptation by conferring novel functionality on the recipient genome[18-22] and reducing competition between clones that carry different beneficial mutations (clonal interference). On the other, owing to the small average size of HGT transfer events and their relatively low rate, it is also likely to introduce disharmonious allele-combinations that will be discriminated against by selection[19].

The balance of these two effects is likely to be different for core and non-core HGT events. Non-core events, such as the introduction of accessory antibiotic resistance genes, can be immediately beneficial and, as they do not replace extant sequence, need not break epistatic interactions. By contrast, HGT replacing one allele for another in part of the core genome is unlikely to introduce great novelty but is likely to disrupt highly evolved co-adapted networks. For these reasons, negative epistatic interactions between core genes with different evolutionary histories have been proposed as a barrier to recombination[4-10, 23], particularly between species.

As bacteria typically have very high effective population sizes and hence efficient selection, the expectation would be that HGT affecting core genes would then be selected against[19]. However,

116 interspecies recombination is common in bacterial core genomes[18, 24]. How, then, can a core
117 genome, that is expected to build up extensive co-adapted epistatic networks, be so accepting of
118 HGT events?
119
120 The common animal gut bacterium *Campylobacter*, which is among the most prolific causes of
121 human bacterial gastroenteritis worldwide[25], provides an exceptional model system to study the
122 impact of HGT on the core genome for several reasons. Introgression between the two most
123 important pathogenic species, *C. jejuni* and *C. coli*, has led to the evolution of a globally
124 distributed 'hybrid' *C. coli* lineage[26] that is responsible for almost all livestock and human
125 infections with this species. Up to 23% of the core genome of common *C. coli* has been recently
126 introgressed from *C. jejuni*[27], potentially disrupting epistatic interactions. As *C. jejuni* and *C. coli*
127 have undergone an extended period of independent evolution (85% average nucleotide identity),
128 recombined sequence is conspicuous in the genome.
129
130 Here, we investigate the disruptive effect of HGT on co-adapted bacterial core genomes by
131 examining covarying allele pairings and imported DNA fragments. Even though recombined
132 fragments enter the genome one-by-one, we find that most covariation in the core genome is
133 between sites where both alleles were imported. Having confirmed that allelic covariation is
134 indicative of epistasis, with laboratory mutagenesis and complementation assays, we conclude
135 that independent disruptive recombination events occur and persist until a second event restores
136 the functional link in a new genetic background. This process resembles the two-hit cancer
137 model. Both bacterial and cancer cell lines are asexual clones and a two-hit model for core
138 genome HGT is consistent with a more general theory in which, whether by multiple mutations

or multiple HGT events, immediate harmful effects from an initial event need not preclude adaptive evolution.

Results

Campylobacter populations are highly structured with intermediate sequence clusters

Analysis every automatically annotated gene from every genome, revealed a core genome of 631 gene orthologues in all *Campylobacter* isolates in this study. There were 1287 genes common to all *C. jejuni* isolates and 895, 1021 and 1272 common to *C. coli* clades 1, 2 and 3, respectively. Consistent with previous studies [27], neighbour-joining and ClonalFrameML trees based on genes within concatenated core genome alignments revealed population structure in which *C. jejuni* and *C. coli* clade 2 and 3 isolates each formed discrete clusters (Figure 1A, Figure S1). Isolates designated as *C. coli* clade 1 were found in three clusters on the phylogeny: unintrogressed ancestral strains, and the ST-828 and ST-1150 clonal complexes (CCs) which account for the great majority of strains found in agriculture and human disease[27]. Pan-genome analysis quantified the increase in unique gene discovery as the number of sampled genomes increased (Figure S2A). For all sequence clusters there was evidence of an open pan-genome with a trend towards continued rapid gene discovery within sequence clusters with fewer isolates. There was considerable accessory genome variation between species and clades, potentially associated with important adaptive traits (Figure S3) and there was evidence that the average number of genes per genome was greater in *C. coli* CC-828 isolates than in *C. jejuni* (Figure S2B).

There is substantial introgression within the *C. coli* core genome

The large genetic distances among *C. coli* clade 1 isolates (Figure 1A), have been shown to be a consequence of the import of DNA from *C. jejuni* rather than accumulation of mutations during a prolonged period of separate evolution[26]. Using chromosome painting to infer the co-ancestry of core-genome haplotype data from CC-828 and CC-1150 isolates gave a detailed representation of the recombination-derived chunks from each *C. jejuni* donor group and clonal complex to each recipient individual (Figure S4). The majority of introgressed SNPs were rare, occurring in fewer than 50 recipient genomes (Figure 1B). However, a large proportion of the introgressed *C. coli* clade 1 genomes contained DNA of *C. jejuni* ancestry in >98% of recipient isolates. Consistent with previous estimates[27], these regions where introgressed DNA was largely fixed within the *C. coli* population, occurred across the genome and comprised up to 15% and 28% of the CC-828 and CC-1150 isolate genomes respectively (Figure 1B). When considering donor groups, the majority of introgressed DNA in *C. coli* involves genes that are present in multiple *C. jejuni* lineages (core genes) (Figure S5A).

Having identified *C. jejuni* ancestry within *C. coli* genomes, we investigated the sequence of events responsible for introgression. Most introgressed SNPs are found at low frequency in both clonal complexes. However, there was evidence of SNPs that are introgressed in both complexes as well as high frequency lineage specific introgression in both CC-828 and CC-1150 (Figure S5B). Specifically, 25% of the *C. jejuni* DNA found in >98% of CC-828 isolates was also found in CC-1150 (Figure S5C), implying that this genetic material was imported by the common ancestor(s) of both complexes. After the divergence of these two complexes, introgression continued with nearly 75% of *C. jejuni* DNA present in one recipient clonal complex and not the other. This is consistent with an evolutionary history in which there was a period of progressive

185 species and clade divergence reaching approximately 12% at the nucleotide level
186 between *C. jejuni* and *C. coli* and around 4% between the three *C. coli* lineages. More recently,
187 changes to the patterns of gene flow led one *C. coli* clade 1 lineage to import substantial
188 quantities of *C. jejuni* DNA, and further lineage-specific introgression gave rise to two clonal
189 complexes (CC-828 and CC-1150) that continued to accumulate *C. jejuni* DNA, independently
190 creating the population structure observed today (Figure 1C).
191
192 The high magnitude introgression into *C. coli* clade 1 isolates has introduced thousands of
193 nucleotide changes to the core genome. However, divergence in bacteria may be uneven across
194 the genome for at least two reasons. First, recombination is more likely to occur in regions where
195 donor and recipient genomes have high nucleotide similarity[24, 28, 29]. Second, 'fragmented
196 speciation'[30], in which gene flow varies in different parts of the genome, such as regions
197 responsible for adaptive divergence, can result in phylogenetic incongruence among genes.
198 Consistent with previous estimates[27], we found that the three *C. coli* clades had similar high
199 divergence with *C. jejuni* across the genome, ranging from 68% to 98% nucleotide identity for
200 individual genes (Figure S5D), implying a period of divergence with low levels of gene flow.
201 We found no evidence that high genetic differentiation between the species prevented
202 recombination. While there was some evidence that more recombination occurred in regions of
203 low nucleotide divergence (between unintrogressed *C. coli* clade 1 and *C. jejuni*), introgression
204 occurred across the genome at sites with varying levels of nucleotide identity (Figure S5D). This
205 level of recombination has greatly increased overall genetic diversity across the genome
206 in *C. coli* clade 1 and introduced changes that have potential functional significance.
207

Much of the putative epistasis occurs between SNPs in introgressed genes

ClonalFrameML analysis revealed the importance of homologous recombination in generating sequence variation within the introgressed *C. coli*. Estimates of the relative frequency of recombination versus mutation (R/θ=0.43), mean recombination event length (δ=152bp) and average amount of polymorphism per site in recombined fragments (ν=0.07), imply that recombination has had an effect (*r/m*) 4.57 times higher than *de novo* mutation during the diversification of CC-828. This is consistent with previous analysis and confirmed recombination as the major driver of molecular evolution in *C. coli*[13, 27, 31]. The continuous time Markov chain model for the joint evolution of pairs of biallelic sites on a phylogenetic tree (Figure S6) was applied to investigate patterns of covariance for all pairs of sites >20kb apart (Figure 2A). For most biallelic sites there were few branches on the tree where substitutions occurred, so that their evolution is compatible with separate evolution on the same clonal frame. However, 2874 covarying pairs evolved more frequently together than would be expected (*p*-value 10^{-8}) if they had evolved independently based on the tree, and hence indicated patterns of putative epistasis.

Among them, the location of 2618 putative epistatic pairs of sites was compared to the inferred ancestry (unintrogressed *C. coli* or *C. jejuni*) of sequence across the genome of CC-828 and CC-1150 *C. coli* strains (Figure 2B, Data S1). For each epistatic pair, the major and minor haplotype were defined if there was haplotype polymorphism between *C. jejuni* and CC-828 and CC-1150 *C. coli*. This allowed quantification of the number of covarying sites that occurred between an ancestral *C. coli* (unintrogressed) and an introgressed *C. jejuni* allele, two introgressed alleles, and sites that do not segregate by species. Strikingly, the breakdown of the major and minor haplotype combinations among the 2618 epistatic pairs (Figure 2C, Data S2) shows the major

231 haplotype for 83.5% of putative epistatic SNP pairs was *C. jejuni* indicating that both co-varying
232 sites had *C. jejuni* ancestry, consistent with epistasis between introgressed ancestral *C. jejuni*
233 sequence at divergent genomic positions. Investigation of the genes containing co-varying sites
234 revealed that 2187 SNP pairs were in 16 genes with just five genes accounting for 99.1% of them
235 (Figure 2D, Data S3, Figure S7).
236
237 **Genomic context and physiological role of epistatically linked genes**
238 The five genes accounting for the majority of epistatic interactions (*cj1167*, *cj1168c*,
239 *cj1171c*/*ppi*, *cj1507c*/*modE* and *cj1508c*/*fdhD*) were investigated for their physiological role in
240 *C. jejuni*. FdhD and ModE are proteins involved in the biogenesis of formate dehydrogenase
241 (FDH). The FDH complex (FdhABC) oxidises formate to bicarbonate to generate electrons that
242 fuel cellular respiration. Formate is an abundant electron donor produced by host microbiota and
243 an important energy source for *Campylobacter in vivo*[32, 33]. The remaining three genes, *cj1167*
244 (annotated incorrectly as *ldh*, lactate dehydrogenase), *cj1168c* and *cj1171c* (*ppi*) are also grouped
245 together in the genome, where *cj1167* and *cj1168c* are adjacent but with the open reading frames
246 (ORFs) convergent and overlapping, while *ppi* is upstream, separated by two non-epistatically
247 linked genes (*cj1169c* and *cj1170c*, Figure 3A). Considering the genomic arrangement, it is
248 therefore clear that the putative epistatic links uncovered in this study essentially occur across
249 two loci in the genome (*fdhD*/*modE* and *cj1167*/*cj1168c*/*ppi*), with each of the latter three genes
250 linked with both *fdhD* and *modE* (Figure 3A). Given the known function of *fdhD* and *modE* in
251 biogenesis of the FDH complex, we hypothesised that *cj1167*/*cj1168c*/*ppi* might also have some
252 role in FDH biogenesis or activity in order to form a functional epistatic connection. We

253 therefore constructed deletion mutants to investigate the possible role of these genes in FDH
254 activity.
255
256 Initially, each of the mutants and their parental wildtype (*C. jejuni* NCTC11168) were grown in
257 rich media (Muller-Hinton broth) and their formate dependent oxygen consumption rates
258 determined (Figure 3B). *cj1167, cj1168c* and *ppi* mutants demonstrated wildtype levels of FDH
259 activity, while activity in both *fdhD* and *modE* mutants was abolished. To confirm that the
260 phenotype of the *fdhD* and *modE* mutants was not due to a polar effect on the surrounding *fdh*
261 locus, these mutants were genetically complemented by reintroduction of a second copy of the
262 wildtype gene into the rRNA locus, which restored near wildtype levels of FDH activity in both
263 cases (Figure 3B).
264
265 As neither *cj1167, cj1168c* or *ppi* mutants showed altered FDH activity in cells grown in rich
266 media, we considered that their function may be related to an FDH-specific nutrient requirement
267 as would likely be found *in vivo*. Since the formate oxidising subunit of FDH, FdhA, specifically
268 requires a molybdo- or tungsto-pterin (Mo/W) cofactor and a selenocysteine (SeC) residue for
269 catalysis[34], Mo, W or Se supply presented possible targets. *cj1168c* encodes a DedA family
270 integral membrane protein of unknown function. DedA proteins are solute transporters
271 widespread in bacteria but are mostly uncharacterised[35]. However, a homologue of *cj1168c* in
272 the heavy metal specialist beta-proteobacterium *Cupriavidus metallidurans* has been shown to be
273 involved in selenite (SeO_3^{2-}) uptake[36]. We therefore speculated that Cj1168 could be a selenium
274 oxyanion transporter that supplies Se for SeC biosynthesis. To test this, FDH activities were
275 measured in *cj1168c* mutant and parental wildtype strains grown in minimal media with limiting

concentrations of selenite or selenate (SeO_4^{2-}) (Figure S8). The data in Figure 3C shows that the *cj1168c* mutant displayed significantly reduced FDH activity after growth with selenite in the low nM range, and this phenotype was partially restored by genetic complementation. We therefore designated *cj1168c* as *selF* (selenium transporter for formate dehydrogenase). However, although this phenotype does suggest that SelF is a selenium importer, another unrelated selenium transporter, FdhT (Cj1500), has previously been documented in *C. jejuni* [37], which is not epistatic with *fdhD* or *modE*. In contrast to this previous report we found considerable residual FDH activity still remained in an *fdhT* deletion mutant, which was fully restored to wildtype levels by complementation (Figure 3D).

Finally, we tested whether the residual FDH activity in our *fdhT* mutant was due to selenium uptake by SelF. An *fdhT selF* double mutant was generated and assayed for FDH activity after growth in minimal media containing limiting concentrations of selenite or selenate (Figure 3D). The *fdhT selF* double mutant demonstrated a significant additional reduction in FDH activity over the *fdhT* single mutant, a phenotype that was partially restored by complementing the double mutant with *selF*. Complementation of the double mutant with *fdhT* returned FDH activity to near wildtype levels (Figure 3D). Taken together, our data suggests that both FdhT and SelF facilitate selenium acquisition in *C. jejuni*, possibly representing low and high affinity transporters, respectively (Figure S9).

Discussion

298 To address the apparent contradiction of frequent core genome recombination in a co-adapted
299 background we focused on *Campylobacter*, in which interspecies recombination is well
300 documented[26, 27, 38]. As in other studies, we found that a large proportion (15-28%) of the *C. coli*
301 core genome originated in *C. jejuni* despite the genetic distance (~85% nucleotide identity)
302 between the species. Investigating the likely disruptive impact on coadapted epistatic gene
303 networks, we quantified the frequency of *C. jejuni – C. coli* (and *vice versa*) and *C. jejuni – C.*
304 *jejuni* covarying allele pairs in introgressed *C. coli*. Where recombination is minimally disruptive
305 there would be more *C. jejuni – C. coli* than *C. jejuni – C. jejuni*. However, consistent with
306 selection against disharmonious gene combinations we found that *C. jejuni – C. jejuni* allele
307 pairs constituted >83% of covarying introgressed haplotypes. It is possible that in some cases
308 both sites were introgressed in a single large recombination event[39-41] but in *Campylobacter* LD
309 for pairs of sites decreases with distance and is approximately constant after 20kbp[42] consistent
310 with the independent acquisition of allele pairs (>20kb). It follows, therefore, that the first
311 introgression event was not fatal to the recipient genome. Acquisition of the second member of
312 the pair then potentially restored the function of the integrated *C. jejuni – C. jejuni*
313 coevolutionary unit.
314
315 Coadaptation and epistasis were confirmed for the most common co-varying *C. jejuni – C. jejuni*
316 gene pairs linked to FDH, a key enzyme allowing the utilisation of formate as an electron donor
317 *in vivo*[32, 33]. FdhD and ModE were shown to be essential for FDH activity. While FdhD is a
318 sulfur-transferase known to be required for the insertion of the pterin cofactor into FdhA[43]
319 (Figure S9), ModE is a transcriptional repressor that has been shown previously only to regulate
320 the Mo/W uptake genes *mod* and *tup*[44, 45]. However, the unexpected abolished FDH activity in a

modE mutant indicates further functions for ModE in FDH biogenesis which warrant future investigation. Searching for functional links between *fdhD*/*modE* and *cj1167*/*selF*/*ppi*, revealed that a *selF* mutant strain had significantly reduced FDH activity under conditions of selenite limitation, a phenotype consistent with SelF being a Se oxyanion transporter and that functionally links SelF with FdhD/ModE. We suggest that *selF* rather than *fdhT* is epistatic because SelF confers an additional benefit for SeC biosynthesis (essential for FDH activity) under conditions of selenium limitation, for example as may be found in the host (Figure S9). *cj1167* encodes a cytoplasmic NADPH dependent 2-oxoacid dehydrogenase but the current genome database annotation as lactate dehydrogenase (Ldh) is incorrect and its function is unknown[46]. There is no precedent for the involvement of such an enzyme in bacterial FDH or SeC biogenesis and we obtained no evidence for a functional connection between Cj1167 and FDH activity. However, the overlapping convergent gene arrangement of *cj1167* and *cj1168c* (*selF*) suggests a transcriptional architecture that might dictate these genes both form similar epistatic dependencies even if Cj1167 is not required for FDH activity. Finally, *cj1171c* (*ppi*) encodes a cytoplasmic peptidyl-prolyl *cis-trans* isomerase of the cyclophilin family. PPIases are general protein folding catalysts that often have pleiotropic and redundant functions[47] and we note that our *C. jejuni ppi* deletion mutant showed no growth defect as well as no reduction in FDH activity. It is possible that if Cj1171 does help promote the folding of e.g. FdhD or ModE, analysis of a simple deletion mutant may not reveal this if another PPIase can substitute in that genetic background.

Understanding the functional significance of core genome recombination has potential to explain the evolution of complex phenotypes. In *Campylobacter*, our results suggest that an ancestral *C.*

coli lineage colonized a new niche and surviving lineages (CC-828 and CC-1150) gained access to *C. jejuni* DNA (Figure 4A&B). As the adaptive landscape of the genome changed, potentially decoupling epistatic interactions that were previously selected, new gene combinations could be introduced by homologous recombination and tested in the *C. coli* genetic background.

The notion that multiple events are necessary to achieve a phenotype with the first event potentially being deleterious (causing negative epistatsis) is strongly reminiscent of the two-hit cancer model in eukaryotes[48] in which the benefit to the tumour cell appears only after earlier non-advantageous mutations. In bacteria, while the first hit (HGT event) in a core genome, is consistent with fitness costs associated with negative epistasis (breaking co-adapted gene networks), this can be rescued by a second HGT event. The second event, in effect restores a pre-existing co-adapted allele pair from the donor species to the recipient. This type of genetic rewiring may indeed be more common than previously thought [49-51] and, despite theoretical expectations, negative epistasis is not an absolute barrier to genome-wide recombination in structured bacterial populations. Multiple HGT events thus provide a solution to the peak jumping problem.

Materials and Methods

Isolates, genome sequencing and assembly

A total of 973 isolates were used in this study, 827 from *C. coli* and a selection of 146 from a diversity of *C. jejuni* clonal complexes (Data S4). Isolates were sampled mostly in the United

Kingdom to maximise environmental and riparian reservoirs and thus the representation of genetic diversity in *C. coli*. Isolates were stored in a 20% (v/v) glycerol medium mix at -80°C and subcultured onto *Campylobacter* selective blood-free agar (mCCDA, CM0739, Oxoid). Plates were incubated at 42°C for 48 h under microaerobic conditions (5% CO2, 5% O2) generated using a CampyGen (CN0025, Oxoid) sachet in a sealed container. Subsequent phenotype assays were performed on Brucella agar (CM0271, Oxoid). Colonies were picked onto fresh plates and genomic DNA extraction was carried out using the QIAamp® DNA Mini Kit (QIAGEN; cat. number: 51306) according to the manufacturer's instructions. DNA was eluted in 100–200 µl of the supplied buffer and stored at −20°C. DNA was quantified using a Nanodrop spectrophotometer and high-throughput genome sequencing was performed on a MiSeq (Illumina, San Diego, CA, USA), using the Nextera XT Library Preparation Kit with standard protocols involving fragmentation of 2 µg genomic DNA by acoustic shearing to enrich for 600 bp fragments, A-tailing, adapter ligation and an overlap extension PCR using the Illumina 3 primer set to introduce specific tag sequences between the sequencing and flow cell binding sites of the Illumina adapter. DNA cleanup was carried out after each step to remove DNA < 150 bp using a 1:1 ratio of AMPure® paramagnetic beads (Beckman Coulter, Inc., USA). Short read paired-end data was assembled using the *de novo* assembly algorithm, SPAdes (version 3.10.0)[52]. All novel genome sequences (n=475) generated for use in this study are available on NCBI BioProjects PRJNA689604 and PRJEB11972. These were augmented with 498 previously published genomes and accession numbers for all genomes can be found in Data S4[16, 27, 31, 42, 53-57].

Genome archiving, pan-genome content analyses and phylogenetic reconstruction

Contiguous genome sequence assemblies were individually archived on the web-based database platform BIGSDB[58] and sequence type (ST) and clonal complex (CC) designation were assigned based upon the *C. jejuni* and *C. coli* multi-locus sequence typing scheme[59]. To examine the full pan-genome content of the dataset, a reference pan-genome list was assembled as previously described[60]. Briefly, genome assemblies from all 973 genomes in this study were automatically annotated using the RAST/SEED platform[61], the BLAST algorithm was used to determine whether coding sequences from this list were allelic variants of one another or 'unique' genes, with two alleles of the same gene being defined as sharing >70% sequence identity on >10% of the sequence length. The prevalence of each gene in the collection of 973 genomes was determined using BLAST with a positive hit in a genome being defined as a local alignment of the reference sequence with the genomic sequence of >70% identity on >50% of the length, as previously described[62]. The resulting matrix was analysed for differentiating core and accessory genome variation. Genes present in all genomes were concatenated to produce a core-genome alignment, used for subsequent phylogenetic reconstructions. Phylogenetic trees were reconstructed using an approximation of maximum-likelihood phylogenetics in FastTree2[63]. This tree was used as an input for ClonalFrameML[64] to produce core genome phylogenies with branch lengths corrected for recombination.

Inference of introgression

All 973 genomes were aligned to a full reference sequence of *C. coli* strain CVM29710. We conducted imputation for polymorphic sites with missing frequency ≤10% using BEAGLE[65] as previously reported[66]. A total of 286,393 gapless SNPs (~17% of the average *C. coli* genome size) were used for recombination analyses. The coancestry of genome-wide haplotype data was

inferred based on alignments using chromosome painting and FineStructure[67] as previously described[68]. Briefly, ChromoPainter was used to infer chunks of DNA donated from a list of 33 donor groups normalised for sample size to each of 677 ST-CC-828 and 12 CC-1150 recipient haplotypes. Results were summarised into a coancestry matrix containing the number of recombination-derived chunks from each donor to each recipient individual. FineStructure was then used for 100,000 iterations of both the burn-in and Markov chain Monte Carlo chain to cluster individuals based on the co-ancestry matrix. The results are visualized as a heat map with each cell indicating the proportion of DNA "chunks" (a series of SNPs with the same expected donor) a recipient receives from each donor.

Analysis of covariation in bacterial genomes

Non-random allele associations can result from selection and clonal population structure. To control for the latter, our approach identified SNP combinations in independent genetic backgrounds by accounting for the sequence variation associated with the inferred phylogeny. Based on the alignment of 677 genomes of *C. coli* CC-828, a first phylogenetic tree was created using PhyML[69]. ClonalFrameML[64] was then applied to correct the tree by accounting for the effect of recombination, and also to infer the ancestral sequence of each node. Covariance was assessed for pairs of biallelic sites across the genome using a Continuous Time Markov Chain (CTMC) model as follows. Briefly, let *A* and *a* denote the two alleles of the first site and *B* and *b* denote the two alleles of the second site, so that there are four states in total for the pair of sites (*ab*, *Ab*, *aB* and *AB*). The four substitution rates from *A* to *a*, from *a* to *A*, from *B* to *b* and from *b* to *B* are not assumed to be identical, to allow for differences in substitution rates in different parts of the genome and also to allow for non-equal rates of forward and backward substitution

(for example as a result of recombination opportunities). Assuming no epistatic effect between the two sites (ε=1), the model M_0 has four free parameters (α_1, α_2, β_1 and β_2) representing independent substitutions at the two sites. We expand model M_0 with an additional fifth parameter ε>1 into model M_1 which is such that the state *AB* where the first site is allele *A* and the second site is allele *B* is favored relative to the other three sites *ab, aB* and *Ab*. Specifically, the state *AB* has a probability increased by a factor ε^2 in the stationary distribution of the CTMC of model M_1 compared to model M_0.

Both models M_0 (with 4 parameters) and M_1 (with 5 parameters) are fitted to the data using maximum likelihood techniques, where the likelihood is equal to the product for every branch of the tree of the state at the bottom of the branch given the state at the top. The two fitted models M_0 and M_1 are then compared using a likelihood-ratio test (LRT) as follows: since M_0 is nested with M_1, two times their difference in log-likelihood is expected to be distributed according to a chi-square distribution with number of degrees of freedom equal to the difference in their dimensionality, which is one. This LRT returns a *p*-value for the significance of a covariation effect, and a Bonferroni correction is applied to determine a conservative cutoff of significance that accounts for multiple testing. Furthermore, the test is applied only to pairs of sites separated by >20kb to reduce the chance that they were the result of a single recombination event, consistent with estimates of the length of recombined DNA sequence in quantitative bacterial transformation experiments[39, 70] and evidence from *Campylobacter* genome analyses that show that LD for pairs of sites decreases with distance to approximately 20kbp and then remains at the same level for very distant sites[42]. It is still possible of course that rare recombination events would stretch 20kbp[39-41], but for this to have an effect on the analysis of epistasis it would have

to have happened several times for the same pairs of sites against different genomic background which becomes quite unlikely just by chance. This phylogenetically aware approach to testing for covariance presents the advantage to naturally account for both population structure and the effect of recombination[71]. The script implementing this coevolution test is available in R at: https://github.com/xavierdidelot/campy.

Quantifying covariation between recombined and unrecombined genomic regions

The results of the introgression and covariation analyses were combined so that for each pair of significantly covarying SNPs (p-value $<10^{-8}$), haplotype frequency was calculated among the 689 recipient introgressed *C. coli* clade-1 strains as well as among the donor *C. coli* (ancestral) and *C. jejuni* strains, respectively. If the most frequent haplotype of the pair is the same between the donor *C. coli* (ancestral) and *C. jejuni*, it was classified as 'no polymorphism'. Otherwise, if the most frequent haplotype accounted for >90% among the recipients, it was classified as either '*C. jejuni* (>90%)' or '*C. coli* (>90%)' if it was the same as that of donor *C. jejuni* or *C. coli* (ancestral) (inset in Figure 2C). If the most frequent haplotype accounted for ≤90% among the recipients, the top two most frequent haplotypes (written as major and minor haplotype in this manuscript) were indicated as either "*C. jejuni* / *C. coli*", "*C. jejuni* / other", "*C. coli* / *C. jejuni*", "*C. coli* / other", "other / *C. coli*", "other / *C. jejuni*", and "other / other", and the frequency of the major and minor haplotypes were calculated. For example, where the haplotype frequencies were as follows, AA=285, TA=192, TG=181, AG=27, A-=2, --=1, -A=1, AA is the major haplotype, frequency of which is 41.3%

Mutagenesis and complementation cloning

Genes *cj1167*, *cj1168c* (here designated *selF* for selenium transport for formate dehydrogenase), *cj1171c* (*ppi*), *cj1507c* (*modE*), *cj1508c* (*fdhD*) and *cj1500* (*fdhT*) were deleted by allelic exchange mutagenesis, with the majority of the open reading frame replaced by an antibiotic resistance cassette. Mutagenesis plasmids were generated by the isothermal assembly method using the HiFi system (NEB, UK). In brief, flanking regions of target genes were PCR amplified from genomic DNA using primers with adaptors homologous to either the backbone vector pGEM3ZF or the antibiotic resistance cassette (Data S5). pGEM3ZF was linearised by digestion with HincII. The kanamycin and chloramphenicol resistance cassettes were PCR amplified from pJMK30 and pAV35, respectively[72]. Four fragments consisting of linearised pGEM3ZF, antibiotic resistance cassette and 2 flanking regions were combined in equimolar amounts and mixed with 2 x HiFi reagent (NEB, UK) and incubated at 50°C for 1 hour. The fragments combine such that the gene fragments flank the antibiotic resistance cassette, in the same transcriptional orientation, within the vector. Mutagenesis plasmids were transformed into *C. jejuni* NCTC 11168 by electroporation. Spontaneous double-crossover recombinants were selected for using the appropriate antibiotic and correct insertion into the target gene confirmed by PCR screening. For genetic complementation of mutants, genes *cj1168c* (*selF*), *cj1507c* (*modE*), *cj1508c* (*fdhD*) and *cj1500* (*fdhT*) were PCR amplified from genomic DNA, restriction digested with MfeI and XbaI, then ligated into similarly digested pRRA[73] (Data S5). The orientation of insertion allowed the target gene to be expressed constitutively by a chloramphenicol resistance gene-derived promoter within the vector. Complementation plasmids were transformed into *C. jejuni* by electroporation. Spontaneous double-crossover recombinants were selected for using apramycin and correct insertion into the ribosomal locus confirmed by PCR screening.

505

506 **Growth of *C. jejuni***

507 Microaerobic growth cabinets (Don Whitley, UK) were maintained at 42°C with an atmosphere
508 of 10% O_2, 5% CO_2 and 85% N_2 (v/v). *C. jejuni* was grown on Columbia-base agar containing
509 5% v/v defibrinated horse blood. Selective antibiotics were added to plates as appropriate at the
510 following concentrations: 50 µg ml^{-1} kanamycin, 20 µg ml^{-1} chloramphenicol, 60 µg ml^{-1}
511 apramycin. Muller-Hinton (MH) broth supplemented with 20 mM L-serine was used as a rich
512 medium. Minimal medium was prepared from a supplied MEM base (51200-38, Thermo
513 Scientific, UK) with the following additions: 20 mM L-serine, 0.5 mM sodium pyruvate, 50 µM
514 sodium metabisulfite, 4 mM L-cysteine. HCl, 2 mM L-methionine, 5 mM L-glutamine, 50 µM
515 ferrous sulfate, 100 µM ascorbic acid, 1 µM vitamin B12, 5 µM sodium molybdate, 1 µM
516 sodium tungstate. Selenium was then added as appropriate from stocks of sodium selenate or
517 sodium selenite prepared in dH_2O. For assays, cells were washed and suspended in sterile
518 phosphate-buffered saline (PBS, Sigma-Aldrich).

519

520 **Respiration rates with formate**

521 Cells were first grown in MH broth for 12 hours, then washed thoroughly in PBS before
522 inoculating minimal media without an added selenium source. The appropriate concentrations
523 were determined by serial dilution trials and it was subsequently found that *C. jejuni* has a strong
524 preference for selenite over selenate, as equivalent FDH activity requires some 1000-fold greater
525 concentration of selenate than selenite (Figure S8). These cultures were grown for 8 hours before
526 the cells were thoroughly washed again, then used to inoculate further minimal media, with a
527 selenium source added as appropriate, and grown for 10 hours. This passaging was necessary to

remove all traces of selenium from the inoculum, such that control cultures without selenium added had negligible (FDH) activity. Assay cultures were again thoroughly washed before the equivalent of 20 ml at an optical density of 0.8 at 600 nm was finally suspended in 1 ml of PBS. Formate-dependent oxygen consumption by whole cells was measured in a Clark-type electrode using 20 mM sodium formate as electron donor. The electrode was calibrated with air-saturated PBS assuming 220 nmol dissolved O_2 ml^{-1} at 37°C. In the electrode, 200 µl of the dense cell suspension was added to 800 µl air-saturated PBS for a final volume of 1 ml. The chamber was sealed and the suspension allowed to equilibrate for 2 minutes. The assay was initiated by the addition of 20 µl of 1 M sodium formate (prepared in PBS) and the rate of oxygen consumption recorded for 90 s. The total protein concentration of the cell suspensions was determined by Lowry assay and the specific rate of formate-dependent oxygen consumption expressed as nM oxygen consumed min^{-1} mg^{-1} total protein.

References

1. Ochman, H., Lawrence, J.G., and Groisman, E.A. (2000). Lateral gene transfer and the nature of bacterial innovation. Nature *405*, 299-304.
2. Koonin, E.V., Makarova, K.S., and Aravind, L. (2001). Horizontal gene transfer in prokaryotes: quantification and classification. Annu. Rev. Microbiol. *55*, 709-742.
3. Haldane, J.B. (1964). A defense of beanbag genetics. Perspect Biol Med *7*, 343-359.
4. Bateson, W. (1909). Heredity And Variation In Modern Lights. In Darwin And Modern Science, A.C. Seward, ed. (Cambridge: Cambridge University Press), pp. 85–101.
5. Fisher, R.A. (1918). The correlation between relatives on the supposition of Mendelian inheritance. Trans. R. Soc. Edinb *52*, 399–433.
6. Wright, S. (1931). Evolution in Mendelian populations. Genetics *16*, 97-159.
7. Dobzhansky, T. (1936). Studies on hybrid sterility. II. Localization of sterility factors in *Drosophila pseudoobscura* hybrids. Genetics *21*, 113-135.
8. Dobzhansky, T. (1937). Genetics And The Origin Of Species, (New York: Columbia University Press).
9. Muller, H.J. (1940). Bearing of the *Drosophila* work on systematics. The new systematics, 185-268.
10. Muller, H. (1942). Isolating mechanisms, evolution, and temperature. Biol. Symp. *6*, 71-125.
11. Kimura, M. (1965). Attainment of quasi linkage equilibrium when gene frequencies are changing by natural selection. Genetics *52*, 875-890.
12. Neher, R.A., and Shraiman, B.I. (2009). Competition between recombination and epistasis can cause a transition from allele to genotype selection. Proc. Natl. Acad. Sci. U.S.A. *106*, 6866-6871.
13. Wilson, D.J., Gabriel, E., Leatherbarrow, A.J.H., Cheesbrough, J., Gee, S., Bolton, E., Fox, A., Hart, C.A., Diggle, P.J., and Fearnhead, P. (2009). Rapid evolution and the importance of recombination to the gastroenteric pathogen *Campylobacter jejuni*. Mol. Biol. Evol. *26*, 385-397.
14. Gibson, B., Wilson, D.J., Feil, E., and Eyre-Walker, A. (2018). The distribution of bacterial doubling times in the wild. Proc. R. Soc. B. *285*.
15. Vos, M., and Didelot, X. (2009). A comparison of homologous recombination rates in bacteria and archaea. Isme J *3*, 199-208.
16. Calland, J.K., Pascoe, B., Bayliss, S.C., Mourkas, E., Berthenet, E., Thorpe, H.A., Hitchings, M.D., Feil, E.J., Corander, J., Blaser, M.J., et al. (2021). Quantifying bacterial evolution in the wild: A birthday problem for Campylobacter lineages. PLoS Genet. *17*, e1009829.
17. Arnold, B.J., Gutmann, M.U., Grad, Y.H., Sheppard, S.K., Corander, J., Lipsitch, M., and Hanage, W.P. (2018). Weak epistasis may drive adaptation in recombining bacteria. Genetics *208*, 1247-1260.
18. Sheppard, S.K., Guttman, D.S., and Fitzgerald, J.R. (2018). Population genomics of bacterial host adaptation. Nat. Rev. Genet. *19*, 549-565.
19. Andreani, N.A., Hesse, E., and Vos, M. (2017). Prokaryote genome fluidity is dependent on effective population size. Isme J *11*, 1719-1721.
20. Vos, M., and Eyre-Walker, A. (2017). Are pangenomes adaptive or not? Nature Microbiol. *2*, 1576-1576.
21. Shapiro, B.J. (2017). The population genetics of pangenomes. Nature Microbiol. *2*, 1574-1574.

22. McInerney, J.O., McNally, A., and O'Connell, M.J. (2017). Why prokaryotes have pangenomes. Nature Microbiol. *2*, 17040.
23. Orr, H.A. (1996). Dobzhansky, Bateson, and the genetics of speciation. Genetics *144*, 1331-1335.
24. Fraser, C., Hanage, W.P., and Spratt, B.G. (2007). Recombination and the nature of bacterial speciation. Science *315*, 476-480.
25. Sheppard, S.K., Dallas, J.F., Strachan, N.J., MacRae, M., McCarthy, N.D., Wilson, D.J., Gormley, F.J., Falush, D., Ogden, I.D., Maiden, M.C., et al. (2009). *Campylobacter* genotyping to determine the source of human infection. Clin. Infect. Dis. *48*, 1072-1078.
26. Sheppard, S.K., McCarthy, N.D., Falush, D., and Maiden, M.C. (2008). Convergence of *Campylobacter* species: implications for bacterial evolution. Science *320*, 237-239.
27. Sheppard, S.K., Didelot, X., Jolley, K.A., Darling, A.E., Pascoe, B., Meric, G., Kelly, D.J., Cody, A., Colles, F.M., Strachan, N.J., et al. (2013). Progressive genome-wide introgression in agricultural *Campylobacter coli*. Mol. Ecol. *22*, 1051-1064.
28. Cohan, F.M. (2002). Sexual Isolation And Speciation In Bacteria. In Genetics of Mate Choice: From Sexual Selection to Sexual Isolation. (Springer), pp. 359-370.
29. Ansari, M.A., and Didelot, X. (2014). Inference of the properties of the recombination process from whole bacterial genomes. Genetics *196*, 253-265.
30. Retchless, A.C., and Lawrence, J.G. (2010). Phylogenetic incongruence arising from fragmented speciation in enteric bacteria. Proc. Natl. Acad. Sci. U.S.A. *107*, 11453-11458.
31. Dearlove, B.L., Cody, A.J., Pascoe, B., Méric, G., Wilson, D.J., and Sheppard, S.K. (2016). Rapid host switching in generalist *Campylobacter* strains erodes the signal for tracing human infections. Isme J *10*, 721-729.
32. Weerakoon, D.R., Borden, N.J., Goodson, C.M., Grimes, J., and Olson, J.W. (2009). The role of respiratory donor enzymes in *Campylobacter jejuni* host colonization and physiology. Microb. Pathog. *47*, 8-15.
33. Taylor, A.J., and Kelly, D.J. (2019). The function, biogenesis and regulation of the electron transport chains in *Campylobacter jejuni*: New insights into the bioenergetics of a major food-borne pathogen. Adv. Microb. Physiol. *74*, 239-329.
34. Smart, J.P., Cliff, M.J., and Kelly, D.J. (2009). A role for tungsten in the biology of *Campylobacter jejuni*: tungstate stimulates formate dehydrogenase activity and is transported via an ultra-high affinity ABC system distinct from the molybdate transporter. Mol. Microbiol. *74*, 742-757.
35. Doerrler, W.T., Sikdar, R., Kumar, S., and Boughner, L.A. (2013). New functions for the ancient DedA membrane protein family. J. Bacteriol. *195*, 3-11.
36. Ledgham, F., Quest, B., Vallaeys, T., Mergeay, M., and Covès, J. (2005). A probable link between the DedA protein and resistance to selenite. Res. Microbiol. *156*, 367-374.
37. Shaw, F.L., Mulholland, F., Le Gall, G., Porcelli, I., Hart, D.J., Pearson, B.M., and van Vliet, A.H.M. (2012). Selenium-dependent biogenesis of formate dehydrogenase in *Campylobacter jejuni* is controlled by the *fdhTU* accessory genes. J. Bacteriol. *194*, 3814-3823.
38. Sheppard, S.K., McCarthy, N.D., Jolley, K.A., and Maiden, M.C.J. (2011). Introgression in the genus *Campylobacter*: generation and spread of mosaic alleles. Microbiology *157*, 1066-1074.
39. Croucher, N.J., Harris, S.R., Barquist, L., Parkhill, J., and Bentley, S.D. (2012). A high-resolution view of genome-wide pneumococcal transformation. PLoS Path. *8*, e1002745.
40. He, M., Sebaihia, M., Lawley, T.D., Stabler, R.A., Dawson, L.F., Martin, M.J., Holt, K.E., Seth-Smith, H.M., Quail, M.A., Rance, R., et al. (2010). Evolutionary dynamics of *Clostridium difficile* over short and long time scales. Proc. Natl. Acad. Sci. U.S.A. *107*, 7527-7532.
41. Power, P.M., Bentley, S.D., Parkhill, J., Moxon, E.R., and Hood, D.W. (2012). Investigations into genome diversity of *Haemophilus influenzae* using whole genome sequencing of clinical isolates and laboratory transformants. BMC Microbiol. *12*, 273.
42. Yahara, K., Méric, G., Taylor, A.J., de Vries, S.P., Murray, S., Pascoe, B., Mageiros, L., Torralbo, A., Vidal, A., Ridley, A., et al. (2017). Genome-wide association of functional traits linked with *Campylobacter jejuni* survival from farm to fork. Environ. Microbiol. *19*, 361-380.
43. Arnoux, P., Ruppelt, C., Oudouhou, F., Lavergne, J., Siponen, M.I., Toci, R., Mendel, R.R., Bittner, F., Pignol, D., Magalon, A., et al. (2015). Sulphur shuttling across a chaperone during molybdenum cofactor maturation. Nat. Commun. *6*, 6148.
44. Taveirne, M.E., Sikes, M.L., and Olson, J.W. (2009). Molybdenum and tungsten in *Campylobacter jejuni*: their physiological role and identification of separate transporters regulated by a single ModE-like protein. Mol. Microbiol. *74*, 758-771.

45. Aguilar-Barajas, E., Díaz-Pérez, C., Ramírez-Díaz, M.I., Riveros-Rosas, H., and Cervantes, C. (2011). Bacterial transport of sulfate, molybdate, and related oxyanions. BioMetals *24*, 687-707.
46. Thomas, M.T., Shepherd, M., Poole, R.K., van Vliet, A.H.M., Kelly, D.J., and Pearson, B.M. (2011). Two respiratory enzyme systems in *Campylobacter jejuni* NCTC 11168 contribute to growth on l-lactate. Environ. Microbiol. *13*, 48-61.
47. Ünal, C.M., and Steinert, M. (2014). Microbial peptidyl-prolyl cis/trans isomerases (PPIases): virulence factors and potential alternative drug targets. Microbiology and molecular biology reviews *78*, 544-571.
48. Knudson, A.G., Jr. (1971). Mutation and cancer: statistical study of retinoblastoma. Proc Natl Acad Sci U S A *68*, 820-823.
49. Oren, Y., Smith, M.B., Johns, N.I., Kaplan Zeevi, M., Biran, D., Ron, E.Z., Corander, J., Wang, H.H., Alm, E.J., and Pupko, T. (2014). Transfer of noncoding DNA drives regulatory rewiring in bacteria. Proc. Natl. Acad. Sci. U.S.A. *111*, 16112-16117.
50. Arnold, B., Sohail, M., Wadsworth, C., Corander, J., Hanage, W.P., Sunyaev, S., and Grad, Y.H. (2019). Fine-scale haplotype structure reveals strong signatures of positive selection in a recombining bacterial pathogen. Mol. Biol. Evol. *37*, 417-428.
51. Wadsworth, C.B., Arnold, B.J., Sater, M.R.A., and Grad, Y.H. (2018). Azithromycin resistance through interspecific acquisition of an epistasis-dependent efflux pump component and transcriptional regulator in *Neisseria gonorrhoeae*. mBio *9*, e01419-01418.
52. Bankevich, A., Nurk, S., Antipov, D., Gurevich, A.A., Dvorkin, M., Kulikov, A.S., Lesin, V.M., Nikolenko, S.I., Pham, S., Prjibelski, A.D., et al. (2012). SPAdes: a new genome assembly algorithm and its applications to single-cell sequencing. Journal of computational biology : a journal of computational molecular cell biology *19*, 455-477.
53. Sheppard, S.K., Didelot, X., Meric, G., Torralbo, A., Jolley, K.A., Kelly, D.J., Bentley, S.D., Maiden, M.C.J., Parkhill, J., and Falush, D. (2013). Genome-wide association study identifies vitamin B5 biosynthesis as a host specificity factor in *Campylobacter*. Proc. Natl. Acad. Sci. U.S.A. *110*, 11923-11927.
54. Sheppard, S.K., Cheng, L., Méric, G., de Haan, C.P., Llarena, A.K., Marttinen, P., Vidal, A., Ridley, A., Clifton-Hadley, F., Connor, T.R., et al. (2014). Cryptic ecology among host generalist *Campylobacter jejuni* in domestic animals. Mol. Ecol. *23*, 2442-2451.
55. Pascoe, B., Méric, G., Yahara, K., Wimalarathna, H., Murray, S., Hitchings, M.D., Sproston, E.L., Carrillo, C.D., Taboada, E.N., Cooper, K.K., et al. (2017). Local genes for local bacteria: evidence of allopatry in the genomes of transatlantic *Campylobacter* populations. Mol. Ecol. *26*, 4497-4508.
56. Pascoe, B., Schiaffino, F., Murray, S., Méric, G., Bayliss, S.C., Hitchings, M.D., Mourkas, E., Calland, J.K., Burga, R., Yori, P.P., et al. (2020). Genomic epidemiology of *Campylobacter jejuni* associated with asymptomatic pediatric infection in the Peruvian Amazon. PLoS Negl. Trop. Dis. *14*, e0008533.
57. Mourkas, E., Taylor, A.J., Méric, G., Bayliss, S.C., Pascoe, B., Mageiros, L., Calland, J.K., Hitchings, M.D., Ridley, A., Vidal, A., et al. (2020). Agricultural intensification and the evolution of host specialism in the enteric pathogen *Campylobacter jejuni*. Proc. Natl. Acad. Sci. U.S.A. *117*, 11018-11028.
58. Jolley, K.A., and Maiden, M.C.J. (2010). BIGSdb: scalable analysis of bacterial genome variation at the population level. BMC Bioinformatics *11*, 595.
59. Dingle, K.E., Colles, F.M., Wareing, D.R., Ure, R., Fox, A.J., Bolton, F.E., Bootsma, H.J., Willems, R.J., Urwin, R., and Maiden, M.C. (2001). Multilocus sequence typing system for *Campylobacter jejuni*. J. Clin. Microbiol. *39*, 14-23.
60. Méric, G., Yahara, K., Mageiros, L., Pascoe, B., Maiden, M.C.J., Jolley, K.A., and Sheppard, S.K. (2014). A reference pan-genome approach to comparative bacterial genomics: identification of novel epidemiological markers in pathogenic *Campylobacter*. PLOS One *9*, e92798.
61. Aziz, R.K., Bartels, D., Best, A.A., DeJongh, M., Disz, T., Edwards, R.A., Formsma, K., Gerdes, S., Glass, E.M., Kubal, M., et al. (2008). The RAST server: rapid annotations using subsystems technology. BMC Genomics *9*, 75.
62. Sheppard, S.K., Jolley, K.A., and Maiden, M.C.J. (2012). A gene-by-gene approach to bacterial population genomics: whole genome MLST of *Campylobacter*. Genes *3*, 261-277.
63. Price, M.N., Dehal, P.S., and Arkin, A.P. (2010). FastTree 2 – approximately maximum-likelihood trees for large alignments. PLOS One *5*, e9490.
64. Didelot, X., and Wilson, D.J. (2015). ClonalFrameML: efficient inference of recombination in whole bacterial genomes. PLoS Comp. Biol. *11*, e1004041.
65. Browning, B.L., and Browning, S.R. (2009). A unified approach to genotype imputation and haplotype-phase inference for large data sets of trios and unrelated individuals. Am. J. Hum. Genet. *84*, 210-223.

66. Yahara, K., Furuta, Y., Oshima, K., Yoshida, M., Azuma, T., Hattori, M., Uchiyama, I., and Kobayashi, I. (2013). Chromosome painting *in silico* in a bacterial species reveals fine population structure. Mol. Biol. Evol. *30*, 1454-1464.
67. Lawson, D.J., Hellenthal, G., Myers, S., and Falush, D. (2012). Inference of population structure using dense haplotype data. PLoS Genet. *8*, e1002453.
68. Yahara, K., Didelot, X., Ansari, M.A., Sheppard, S.K., and Falush, D. (2014). Efficient inference of recombination hot regions in bacterial genomes. Mol. Biol. Evol. *31*, 1593-1605.
69. Guindon, S., Dufayard, J.-F., Lefort, V., Anisimova, M., Hordijk, W., and Gascuel, O. (2010). New algorithms and methods to estimate maximum-likelihood phylogenies: assessing the performance of PhyML 3.0. Syst. Biol. *59*, 307-321.
70. Mell, J.C., Shumilina, S., Hall, I.M., and Redfield, R.J. (2011). Transformation of natural genetic variation into *Haemophilus influenzae* genomes. PLoS Path. *7*, e1002151-e1002151.
71. Collins, C., and Didelot, X. (2018). A phylogenetic method to perform genome-wide association studies in microbes that accounts for population structure and recombination. PLoS Comp. Biol. *14*, e1005958.
72. van Vliet, A.H., Wooldridge, K.G., and Ketley, J.M. (1998). Iron-responsive gene regulation in a *Campylobacter jejuni fur* mutant. J. Bacteriol. *180*, 5291-5298.
73. Cameron, A., and Gaynor, E.C. (2014). Hygromycin B and apramycin antibiotic resistance cassettes for use in *Campylobacter jejuni*. PLOS One *9*, e95084.

Acknowledgments

Funding: Wellcome Trust grant 088786/C/09/Z (SS), Medical Research Council (MRC) grant MR/M501608/1 (SS), Medical Research Council (MRC) grant MR/L015080/1 (SS), Food Standards Agency project FS101087 (SS), Biotechnology & Biological Sciences Research Council (BBSRC) grant BB/S014497/1 (DK).

Author contributions:

Conceptualization and study design: SS, XD, DF, KY, DK, AT

Sample collection: SS, AvV, NW

Laboratory work: GM, AT, LM, MH, BP

Data archiving: BP, KJ

Data analysis: AT, XD, KY, LM, JKC, EM, SP, SB, SS, JC

Data interpretation: KY, GM, XD, SS, MM, JP, DK, AT, DF

Writing: SS, GM, BP, CK, AT, DK

Competing Interest Statement: The authors declare that they have no competing interests.

Data and materials availability: Short-read sequence data for all isolates sequenced in this study are deposited in the sequence read archive (SRA) and can be found associated with NCBI BioProjects PRJNA689604 (https://www.ncbi.nlm.nih.gov/bioproject/PRJNA689604) and PRJEB11972 (https://www.ncbi.nlm.nih.gov/bioproject/PRJEB11972). These were augmented with 498 previously published genomes and assembled genomes are available on Figureshare (doi.org/10.6084/m9.Figureshare.13521683). Accession numbers for all genomes are included in Data S4. Source data are provided for this paper (Data S2).

765

766

767

768

769

770

771 **Figureures and Tables**

772

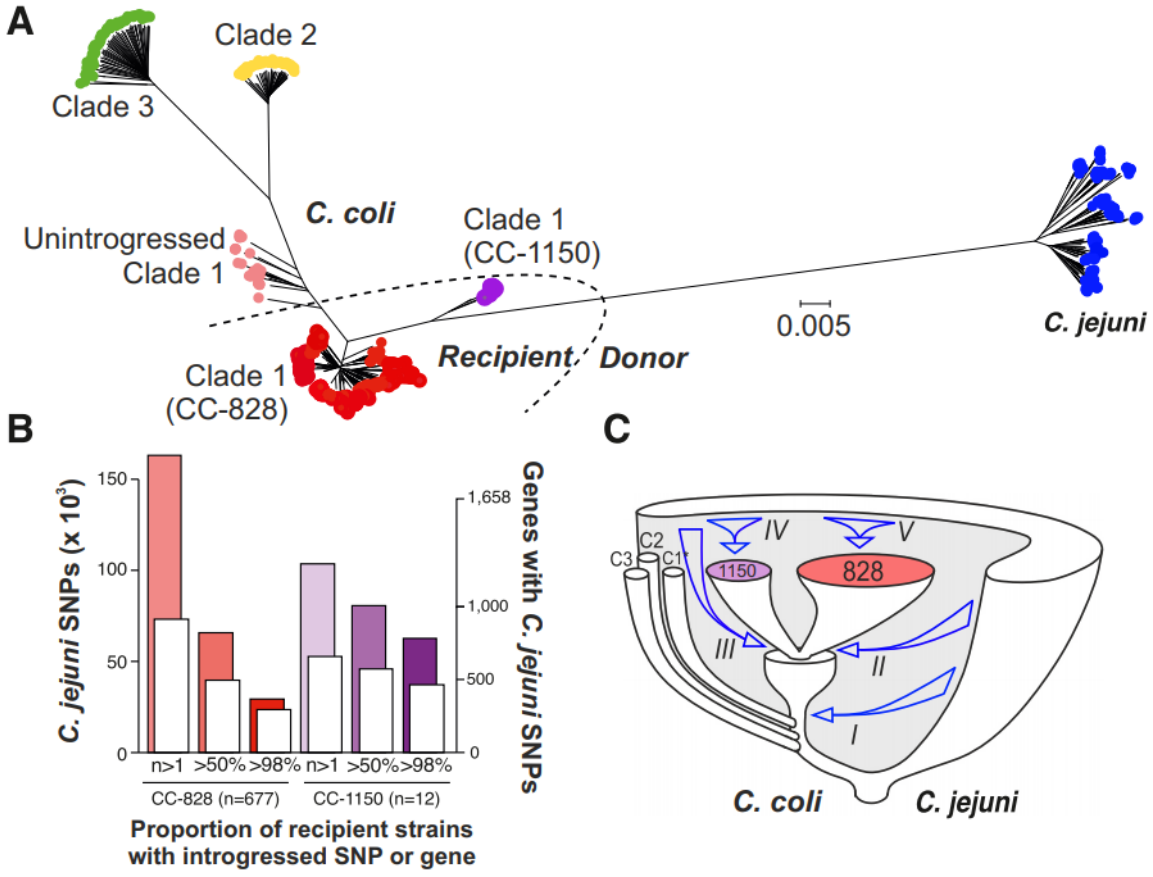

773

774

775 **Figure 1. Genome-wide introgression from *C. jejuni* to *C. coli*.** (A) Phylogenetic tree

776 reconstructed using neighbour-joining on a whole-genome alignment of 973 *C. jejuni* and *C. coli*

777 isolates. Introgressed *C. coli* clades are represented with red (CC-828, n=677) and purple (CC-
778 1150, n=12) circles, unintrogressed clade 1 (n=35) is shown in pink, clade 2 (n=45) in yellow
779 and clade 3 (n=58) in green. A set of 146 *C. jejuni* genomes belonging to 30 clonal complexes (4
780 to 5 isolates per ST) are shown in blue. Recipient and donor populations, used to infer
781 introgression in chromosome painting analysis, are indicated. The scale bar represents the
782 number of substitutions per site. (B) Summary of introgressed *C. jejuni* SNPs in *C. coli* CC-828
783 (n=677, red) and CC-1150 (n=12, purple) genomes using ChromoPainter; the number of
784 introgressed core SNPs (coloured histograms; left y-axis) and core genes (white histograms; right
785 y-axis) for a range of recipient strains proportions (at least 1, more than 50% and more than
786 98%) is shown. (C) Diagram of *Campylobacter* species and clade (C1*, C2, C3) divergence with
787 arrows indicating introgression from *C. jejuni* into *C. coli* (i) clade 1, (ii, iii) CC-828 and CC-
788 1150, (iv, v) subsequent clonal expansion and ongoing introgression.
789

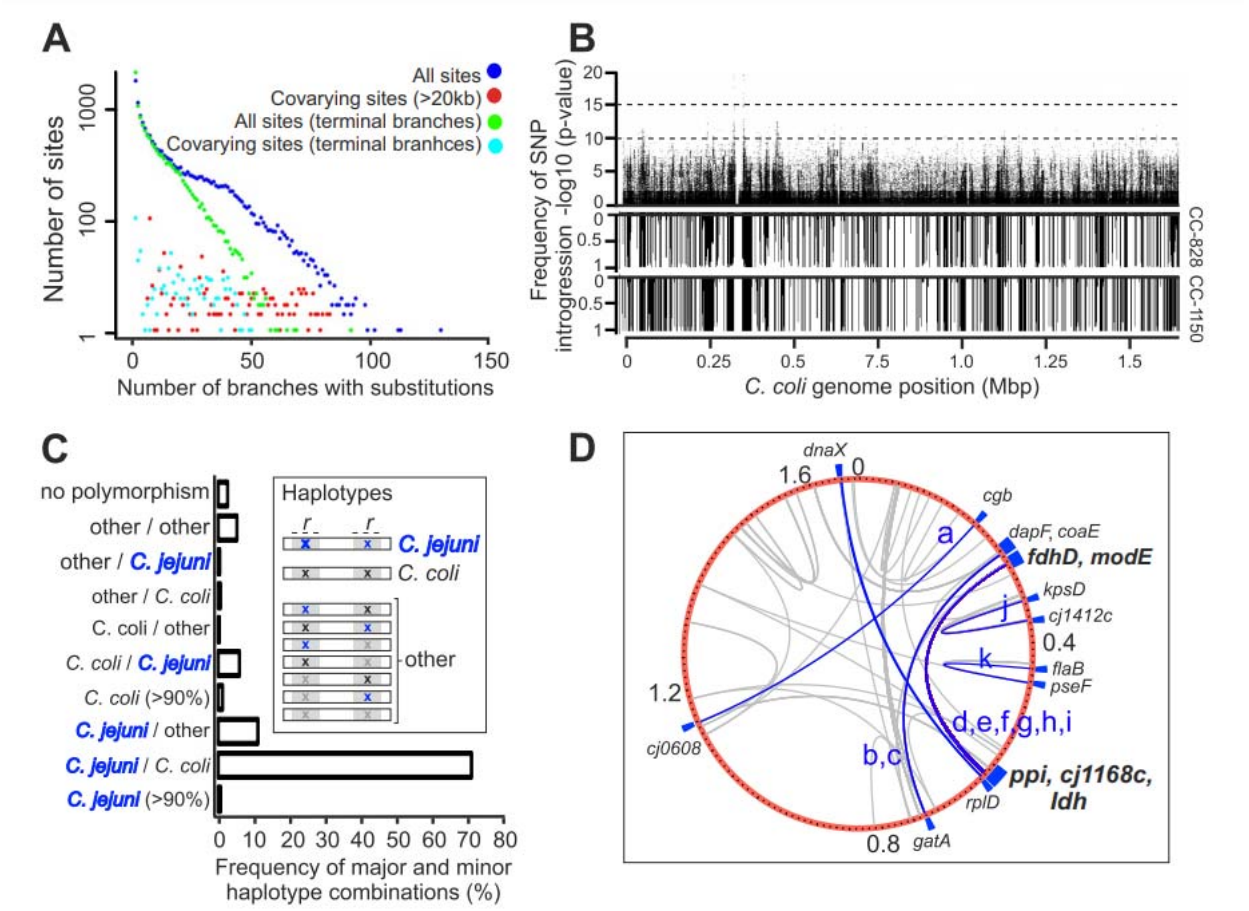

Figure 2. Covariation in introgressed *C. coli* genomes. (A) CC-828 and CC-1150 *C. coli* genomes were analysed using a continuous time Markov chain (CTMC) model and covariation was assessed for pairs of biallelic sites separated by at least 20kb along the genome while accounting for the effect of population structure and recombination. There are many biallelic sites that do not change often on the tree and few that do. Putative epistatic sites change more frequently than average with biallelic pairs found together on multiple branches. (B) Miami plot of each polymorphic site showing the maximum *p*-value for covarying biallelic pairs (>20kb apart) and the frequency of introgression in CC-828 and CC-1150. (C) The frequency of major and minor haplotype combinations (inset) among the 2578 pairs of covarying SNPs in the 689 *C. coli* clade-1 recipient genomes, revealing that the majority of long range covariation was

between introgressed *C. jejuni* sites. (D) The position of putative epistatic sites mapped on the *C. coli* CVM29710 reference for covarying *C. jejuni*-*C. jejuni* SNPs (red) in 16 gene pairs (a to l), and other haplotype combinations (grey).

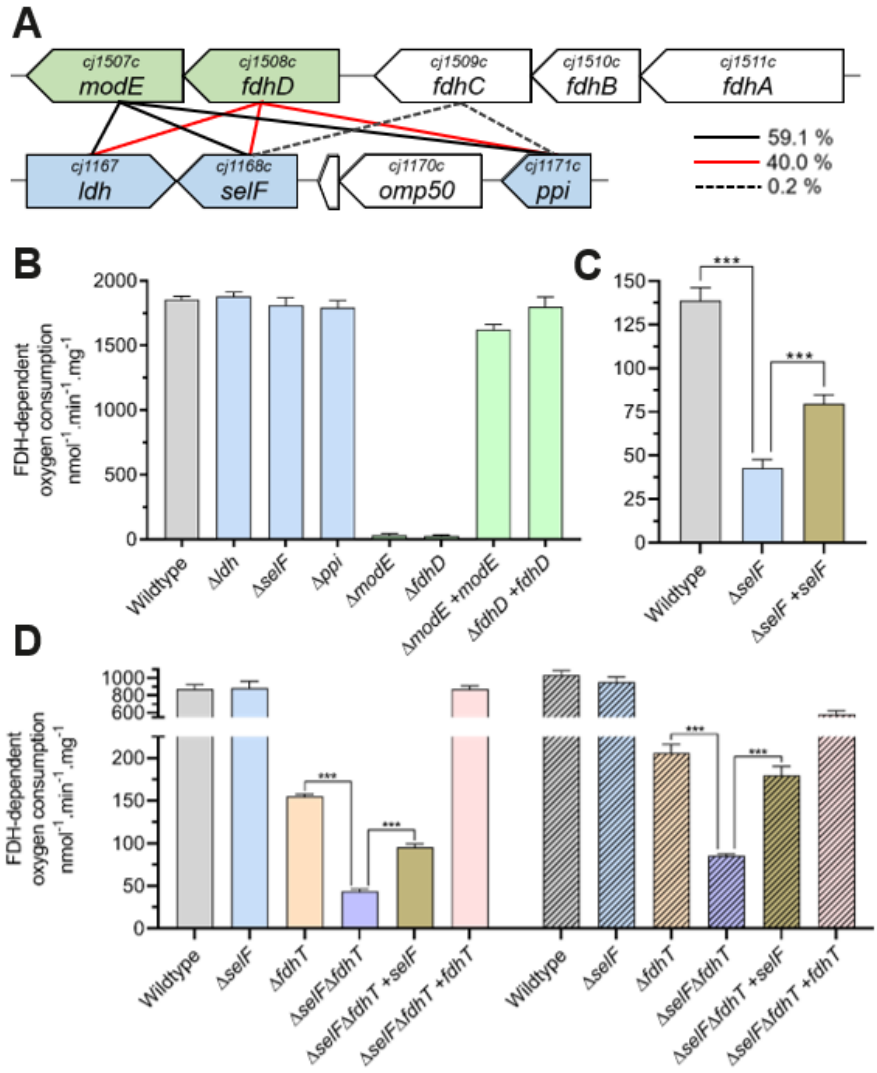

Figure 3. Genomic context and physiological roles of introgressed epistatically linked genes involved in FDH biogenesis and activity. (A) Genome organisation and percentage of co-varying SNP pairs (internal legend). (B-D) FDH activity of whole cells determined by oxygen consumption rates in a Clark-type electrode (nmol oxygen consumed per minute per mg of total protein) for (B) cells grown in rich media (excess selenium), (C) cells grown in minimal media with 0.5 nM sodium selenite, and (D) cells grown in minimal media with either 5 nM sodium selenite (left, open bars) or 5 µM sodium selenate (right, hashed bars). All data are means of at

824 least 4 independent determinations and error bars are SD. *** denotes *p* value of <0.001 by
825 students *t*-test. Assays suggest that both FdhT and SelF facilitate selenium acquisition, possibly
826 representing low and high affinity transporters, respectively.
827
828
829
830
831
832
833
834
835
836
837
838
839
840
841

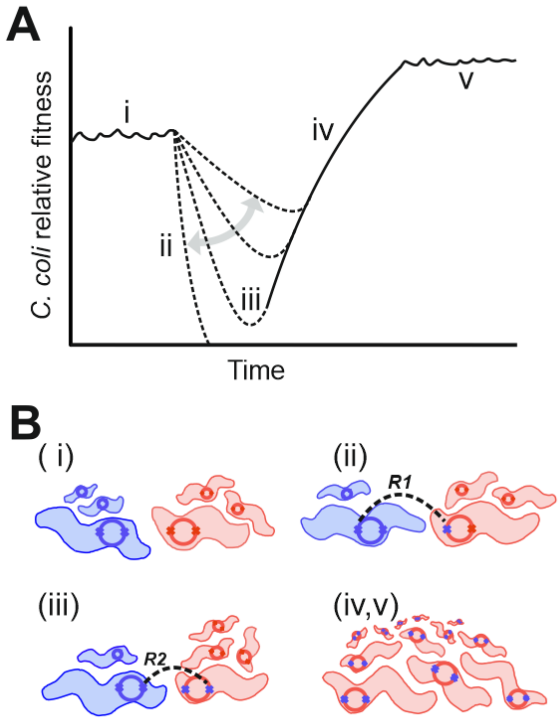

Figure 4. A two-hit model for core genome recombination in natural *C. coli* populations. A&B: (i) *C. jejuni* (blue) and unintrogressed *C. coli* (red) co-exist with genomes (internal circles) harbouring haplotype pairs (x-x) that segregate by species; (ii) Horizontal gene transfer, HGT, occurs (R1) disrupting covarying genetic elements and reducing the relative fitness of introgressed *C. coli* to varying degrees (grey arrow), few strains retain mixed *C. coli* - *C. jejuni* haplotypes; (iii) HGT continues (R2) and, where recombined mixed haplotypes survived, ancestral *C. jejuni* haplotype pairs are reinstated in introgressed *C. coli;* (iv,v) introgressed *C. coli* outcompete unintrogressed strains.